

Mass attenuation coefficient of olive peat material for absorbing gamma ray energy

Mohammad W. Marashdeh¹ · Hanan Saleh²

Received: 26 September 2018 / Revised: 23 November 2018 / Accepted: 22 December 2018 / Published online: 4 June 2019
© China Science Publishing & Media Ltd. (Science Press), Shanghai Institute of Applied Physics, the Chinese Academy of Sciences, Chinese Nuclear Society and Springer Nature Singapore Pte Ltd. 2019

Abstract The mass attenuation coefficients (μ/ρ) of a natural material, i.e., olive peat, were measured at photon energies of 0.059, 0.356, 0.662, 1.17, and 1.332 MeV and compared with those of concrete and Pb. The experimental samples were irradiated with ^{214}Am , ^{133}Ba , ^{137}Cs , and ^{60}Co point sources using a transmission arrangement. The olive peat samples were obtained from different areas in Jordan, namely Mafraq (sample M), Kerak (sample K), Ajloun (sample A), and Irbid (sample I), and photon energies were measured using a NaI(Tl) scintillation detector with an energy resolution of 7.6% at 662 keV. The differences in the μ/ρ of olive peat samples and the calculated μ/ρ of concrete were consistently within 0.7% at photon energies of 0.356–1.332 MeV. This finding indicates that olive peat can be used in radiation applications in the field of medical physics. Finally, the half-value layer (HVL) of the experimental samples was measured, and results were compared with those of concrete and Pb. Pb and concrete exhibited minimal HVL values due to their high density, and the HVL of olive peat revealed lower shielding effectiveness than that of concrete.

Keywords Olive peat · Attenuation coefficient · Half-value layer · Gamma ray

1 Introduction

The search for new alternative sources of energy, especially those that can replace petroleum, is a popular research topic. Jordan experiences increased demands for fuel during winter. As the price of fuel increases, alternative sources of heat energy must be developed. One such potential energy source is olive peat, which is easily dried from flammable materials and can spread heat when used in fireplaces or wood stoves. Olive peat is also an important alternative fuel source in cement and iron factories.

The olive peat can be used as a clean, reliable source of energy [1] and organic compost [2]. Olive peat is commonly used as an energy source instead of firewood because of its low cost, as some prefer it instead of wood to reduce the logging [3]. The use of olive peat reduces the need for logging in forest areas. As Jordan is characterized by large quantities of olive trees [4], peat can easily be acquired during the processing of olives. Peat is all that remains of olive seeds, fruits, and leaves after processing. It is a substance rich in oil, which usually makes up 40% of the weight of the fruit, and can easily be obtained from the residue of olive presses they are grouped with each end of the olive milling season. Exposure to radiation from various natural sources is a daily occurrence. The extent of exposure to natural radiation varies according to one's location, and complete protection against radiation exposure is usually impossible unless specific procedures from appropriate buildings are applied. In general, the use of radiation shielding, the type of shielding applied, and the amount of shielding necessary depend on the type of radiation present and its activity.

Application of gamma rays is rapidly increasing in several fields, such as nuclear and radiation physics,

✉ Mohammad W. Marashdeh
mwmarashdeh@gmail.com; mwmarashdeh@imamu.edu.sa

¹ Department of Physics, College of Sciences, Imam Mohammad Ibn Saud Islamic University (IMSIU), P.O. Box 90950, Riyadh 11623, Saudi Arabia

² Department of Radiography, Princess Aisha Bint Al-Hussein College of Nursing and Health Sciences, Al-Hussein Bin Talal University, P.O. Box 20, Ma'an, Jordan

industry, medicine, environment, energy production, radiation dosimetry, biological physics, and agriculture [5–11]. While Pb is usually applied as a traditional shielding material for radiation, the extensive use of this material is impractical because of its high density and cost. Previous studies have suggested the use of materials, such as concrete, colemanite, steel and polymers, as radiation shields [12–19]. The mass attenuation coefficient (μ/ρ) characterizes the penetration and diffusion of gamma radiation into a material. The half-value layer (HVL) is useful to understand the behavior of a material subjected to ionizing radiation [20, 21].

Olive peat is widely available indoors in Jordan, and knowledge of its radioactive behavior is important to determine whether it can be used as a radiation shield. To date, no previous studies on this material have yet been published. Studying the radiation attenuation coefficient of olive peat material is of considerable interest. The aim of this study is to identify the energy parameters of olive peat and assess its shielding ability. Herein, the μ/ρ of olive peat samples obtained at photon energies of 0.059, 0.356, 0.662, 1.17, and 1.332 MeV is compared with the calculated μ/ρ of concrete and lead.

2 Experimental

2.1 Sample preparation

After the oil had been extracted from olives, the rest of the unused samples were packed in an open area, usually near a water pond, and exposed for approximately 1 month. The samples were collected from different areas in Jordan, namely Mafraq (sample M), Kerak (sample K), Ajloun (sample A), and Irbid (sample I), and left for 30 days in the air to reduce their water content. Figure 1 shows the different locations from which the samples were obtained.

Samples were dried to about 6% moisture and then sieved (size: 140 μm) to remove large particles. They were then compressed into pellets using a manual hydraulic press machine for 45 s at 31 MPa. No other reagent was added to the material to fabricate the binderless pellets. Four pellets of different thickness (i.e., 0.5, 1.0, 1.5, or 2.0 cm) and an area of 1.41 cm^2 were obtained. Table 1 lists the olive peat samples according to the area from where they were obtained and the densities measured after pelletization. The densities of the pellets were calculated by dividing their mass (g) by their volume (cm^3).

Energy-dispersive X-ray analysis (EDXA) (FEI Nova SEM 450) was used to determine the elemental composition of the samples. The pellets were scanned at magnifications of 500 \times and 1000 \times at an acceleration voltage of

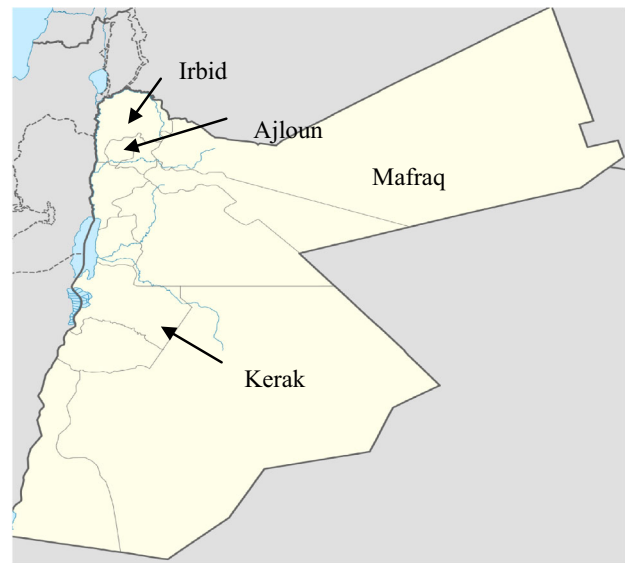


Fig. 1 The sampling sites of olive peat in Jordan

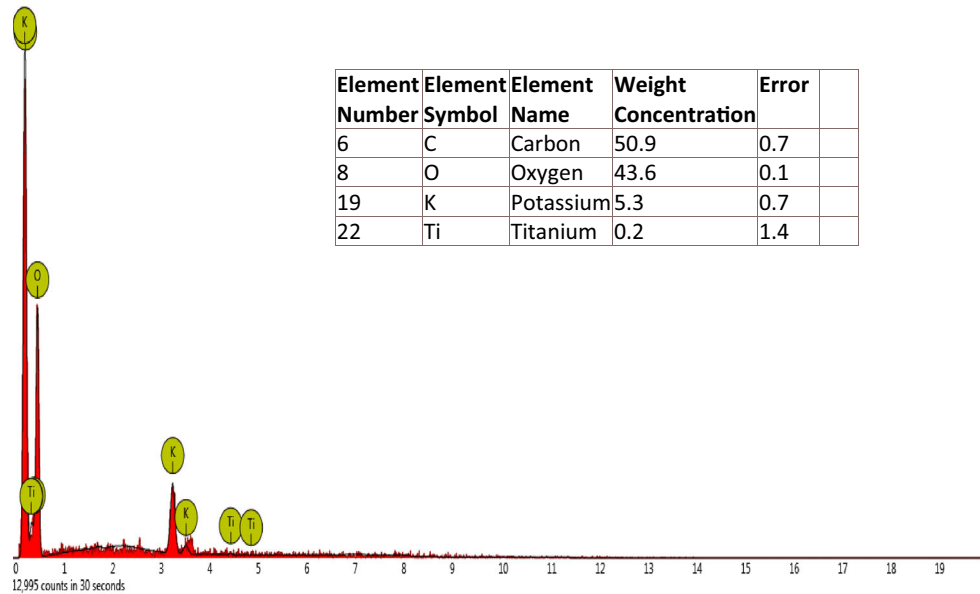
Table 1 Olive peat samples with obtained sampling sites and measured densities

Samples	Sampling sites	Measured density (g/cm^3)			
		Average	Max.	Min.	SD
M	Mafraq	1.21	1.24	1.18	0.03
K	Kerak	1.28	1.31	1.25	0.03
A	Ajloun	1.16	1.18	1.14	0.02
I	Irbid	1.18	1.21	1.15	0.03

10 kV (Fig. 2). Details of the elemental composition of the olive peat samples and the results of chemical analysis of concrete are shown in Table 2.

2.2 Mass attenuation coefficient measurements

The linear mass coefficient (μ) and μ/ρ are determined by measuring the transmission photon beam passing through samples of known thickness. The experimental setup in this work is shown in Fig. 3. Point sources (10 mCi) of ^{214}Am (0.059 MeV), ^{133}Ba (0.356 MeV), ^{137}Cs (0.662 MeV), and ^{60}Co (1.17 and 1.332 MeV) were used to irradiate the samples. Each sample was irradiated thrice, and the average value was taken to calculate μ . Energy intensities were measured using a 2" \times 2" NaI(Tl) scintillation detector (ORTEC Inc.) with an energy resolution of 7.6% at 662 keV. Signals were collected into a spectroscopic amplifier and multichannel pulse height analyzer, and samples were irradiated for 3600 s to ensure good statistics. The gamma spectra were analyzed using a Maestro-ORTEC instrument.

Fig. 2 EDXA spectrum and elemental composition of olive peat made from sample A**Table 2** Elemental composition (%) by relative weight of the olive peat (M, K, A, and I) samples and concrete

	Samples				
	M (%)	K (%)	A (%)	I (%)	Concrete (%)
H	—	—	—	—	0.9
C	54.7	57.7	50.9	52.3	0.1
O	41.2	41.2	43.6	41.3	53.6
K	4.1	—	5.3	—	0.3
Ti	—	—	0.2	3.7	—
In	—	1.1	—	—	—
Na	—	—	—	—	0.5
Mg	—	—	—	—	0.1
Al	—	—	—	—	1.3
Si	—	—	—	—	36.7
S	—	—	—	—	0.1
Fe	—	—	—	—	0.6
Ca	—	—	—	—	5.6

The detector shield was surrounded by a 5-cm-thick layer of Pb to reduce background and scattered radiation. The diameters of the collimator facing the detector and another collimator in front of the point source were 0.3 and 0.5 cm, respectively, and the distances between the point source and sample and between the sample and detector were 8 and 7 cm, respectively. The experimental setup is displayed in Fig. 3.

The μ (cm^{-1}) and μ/ρ (cm^2/g) of the olive peat samples were calculated according to Beer–Lambert's law using Eqs. (1) and (2), respectively.

$$I = I_0 e^{-\mu x}, \quad (1)$$

$$\mu/\rho = \frac{1}{\rho x} \ln \left(\frac{I_0}{I} \right), \quad (2)$$

where I_0 denotes the photon intensity without sample; I is the photon intensity after sample; and ρx is the mass thickness.

The error in the mass attenuation coefficient (μ/ρ) is given by:

$$\sigma_{\mu/\rho} = \left(\frac{\sigma_\mu}{\mu} + \frac{\sigma_\rho}{\rho} \right) \times \left(\frac{\mu}{\rho} \right), \quad (3)$$

where $\sigma_\mu = \pm(\mu_{\max} - \mu_{\min})/2$ and ρ is the density of the sample.

The attenuation experiment was performed by measuring the μ/ρ of Al with a thickness of 0.5 cm (Fig. 4). No significant difference between the theoretical and experimental μ/ρ of Al at different gamma ray energies was observed, and a high correlation of $R^2 = 0.9981$ was obtained. The theoretical μ/ρ of Al was calculated using XCOM software.

2.3 Half-value layer

X-ray penetration through a shielding material is characterized by the attenuation property and half-value layer (HVL). Accurate data of these characteristics are necessary to develop shielding materials for different applications, such as nuclear medicine, radiation physics, and radiology. HVL is defined as the material thickness at which the incident photon intensity falls to half its value ($I_0/2$). The

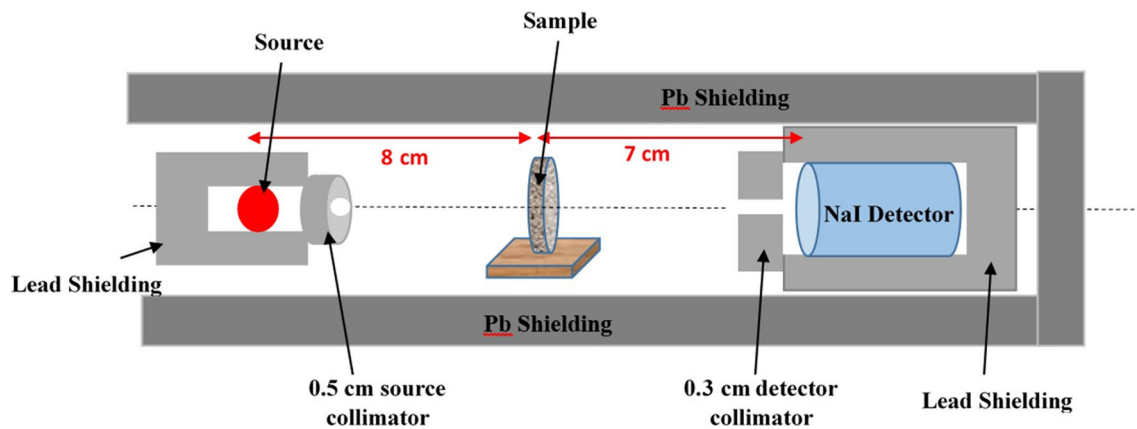


Fig. 3 Experimental setup (color online)

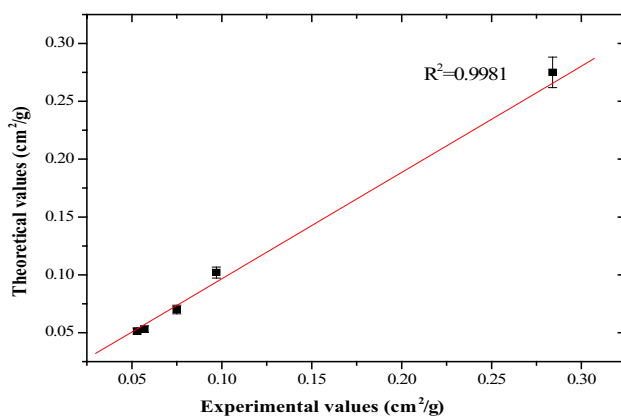


Fig. 4 The comparison of experimental and theoretical values of mass attenuation coefficients of Al

HVL of the olive peat samples is calculated according to Eq. (4).

$$HVL = \frac{\ln 2}{\mu} \quad (4)$$

3 Results and discussion

3.1 Mass attenuation coefficient measurements

The μ/ρ of the olive peat samples obtained at photon energies of 0.059, 0.356, 0.662, 1.17, and 1.332 MeV is shown in Table 3. The intensities of the incident and transmitted gamma rays are determined from the net area under the k_{α} peak of the different sources. The errors in μ/ρ of the olive peat samples are between 0.002% and 0.020%. Table 3 reveals that μ/ρ decreases with increasing photon energy, as also shown in Fig. 5. The difference in measured μ/ρ of the olive peat samples can be attributed to differences in the elemental compositions of the samples.

However, no difference in terms of basic elements, such as oxygen and carbon, which have similar atomic numbers, is found. No significant differences between the μ/ρ of the olive peat samples are observed in the range of 0.356–1.332 MeV, likely due to the similarity of the basic structure of the samples. Clear variations among the samples occur at 0.059 MeV.

The calculated and measured μ/ρ of the olive peat samples is shown in Table 4. Good agreement between the experimental and theoretically calculated results is observed in the range of 0.356–1.332 MeV, but the former tend to be slightly lower than the latter. This difference can be attributed to differences in the elemental compositions of the samples.

Figure 5 compares the experimental μ/ρ of the olive peat samples with the theoretical μ/ρ of concrete and Pb as calculated using XCOM software [22]. The μ/ρ of the olive peat samples is in close agreement with the calculated μ/ρ of concrete. Interestingly, the experimental μ/ρ of the olive peat samples and calculated μ/ρ of concrete and Pb decrease irregularly with increasing photon energy. Photoelectric and Compton effects appear to dominate at energy levels less than 0.356 MeV (Fig. 5). In addition, the different μ/ρ of the four studied samples, concrete, and Pb could be clearly observed in the low-energy region. This result can be attributed to the fact that photoelectric effects are different from varying material combinations of olive peat and concrete materials when compared with Pb material. The olive peat samples contain essential elements, namely O and C, as well as slight differences in some heavy-metal elements; these differences can affect the μ/ρ of the samples at low photon energies. In addition, the olive peat material has the ability to capture these elements, and therefore, future studies can be carried out on this material. Figure 6 shows the experimental μ/ρ of the samples at 0.356–1.332 MeV in comparison with the XCOM-calculated μ/ρ of concrete and Pb. The μ/ρ of the

Table 3 The experimental values of linear and mass attenuation coefficients of olive peat (M, K, A, and I) samples at the photon energy of 0.059, 0.356, 0.662, 1.17, and 1.332 MeV

Samples	^{241}Am			^{133}Ba			^{137}Cs			^{60}Co			^{60}Co		
	0.059 MeV			0.356 MeV			0.662 MeV			1.17 MeV			1.332 MeV		
	μ (cm^{-1})	μ/ρ (cm^2g^{-1})	Error (\pm %)	μ (cm^{-1})	μ/ρ (cm^2g^{-1})	Error (\pm %)	μ (cm^{-1})	μ/ρ (cm^2g^{-1})	Error (\pm %)	μ (cm^{-1})	μ/ρ (cm^2g^{-1})	Error (\pm %)	μ (cm^{-1})	μ/ρ (cm^2g^{-1})	Error (\pm %)
M	0.206	0.169	0.019	0.119	0.096	0.012	0.092	0.073	0.008	0.071	0.056	0.004	0.067	0.052	0.003
K	0.283	0.221	0.020	0.127	0.098	0.017	0.098	0.075	0.006	0.077	0.058	0.005	0.071	0.053	0.003
A	0.235	0.203	0.017	0.112	0.095	0.011	0.088	0.074	0.006	0.068	0.055	0.003	0.064	0.053	0.002
I	0.207	0.175	0.016	0.114	0.094	0.013	0.088	0.074	0.004	0.068	0.056	0.004	0.065	0.054	0.003

Fig. 5 Mass attenuation coefficient at photon energy (0.059–1.133) MeV for olive peat (M, K, A, and I) samples compared with calculated XCOM for concrete and lead

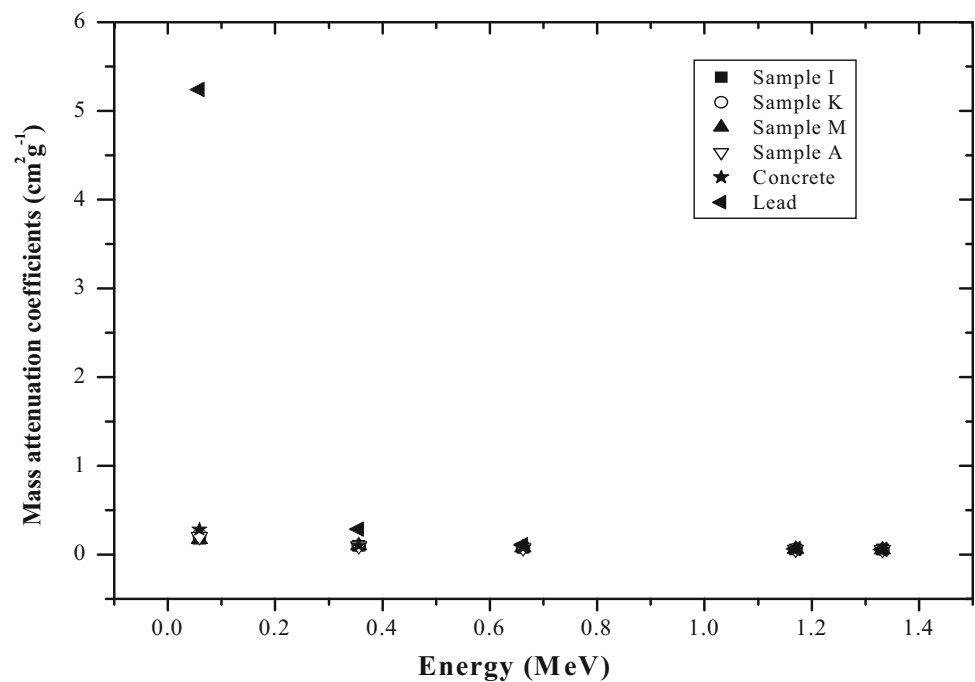


Table 4 Experimentally measured and theoretically calculated (XCOM) mass attenuation coefficients of olive peat (M, K, A, and I) samples at 0.059, 0.356, 0.662, 1.17, and 1.332 MeV photon energies

Samples	^{241}Am		^{133}Ba		^{137}Cs		^{60}Co		^{60}Co	
	0.059 MeV		0.356 MeV		0.662 MeV		1.17 MeV		1.332 MeV	
	Calc.	Exp.	Calc.	Exp.	Calc.	Exp.	Calc.	Exp.	Calc.	Exp.
M	0.185	0.169 ± 0.019	0.100	0.096 ± 0.012	0.077	0.073 ± 0.008	0.060	0.056 ± 0.004	0.055	0.052 ± 0.003
K	0.239	0.221 ± 0.020	0.100	0.098 ± 0.017	0.077	0.075 ± 0.006	0.060	0.058 ± 0.005	0.055	0.053 ± 0.003
A	0.207	0.203 ± 0.017	0.100	0.095 ± 0.011	0.077	0.074 ± 0.006	0.060	0.055 ± 0.003	0.055	0.053 ± 0.002
I	0.192	0.175 ± 0.016	0.099	0.094 ± 0.013	0.077	0.074 ± 0.004	0.060	0.056 ± 0.004	0.055	0.054 ± 0.003

olive peat samples is closer to the calculated μ/ρ of concrete than to the calculated μ/ρ of Pb at 0.0356 MeV. The level of agreement between the attenuation measurements for olive peat and concrete at the studied photon energy range has not been measured in the previous work. These results indicate that olive peat can potentially be used as radiation shield or as a phantom material.

The percentage difference between the experimental μ/ρ of olive peat samples and the calculated μ/ρ of concrete at photon beam energies of 0.059, 0.356, 0.662, 1.17, and 1.332 MeV is shown in Table 5. No significant difference was found among the olive peat samples and the calculated concrete, where the percentage difference of μ/ρ values for olive peat samples from concrete is within 0.7% at photon energies of 0.356–1.332 MeV. However, the radiation behaviors of the same samples were consistent with the previous results [23, 24] at a low photon energy of

0.059 MeV. In addition, the percentage difference in the μ/ρ of sample K from the calculated μ/ρ of concrete was generally lower than that of other samples at all energies tested.

A comparison of the μ/ρ of olive peat samples with those of some polymeric materials by [23–25] is presented in Table 6. The μ/ρ of the olive peat samples at 0.059 MeV is compatible with that of Perspex [23] and polycarbonate [24]. These findings indicate that olive peat has potential use in radiation applications in the field of medical physics.

3.2 Half-value layer (HVL) measurements

The measured HVL of the olive peat samples and calculated HVL of concrete and Pb are given in Table 7. The results indicate that HVL depends on the photon energy. Figure 7 compares the experimental HVL of the samples

Fig. 6 Mass attenuation coefficient at photon energy (0.356–1.133) MeV for olive peat (M, K, A, and I) samples compared with the calculated XCOM for concrete and lead

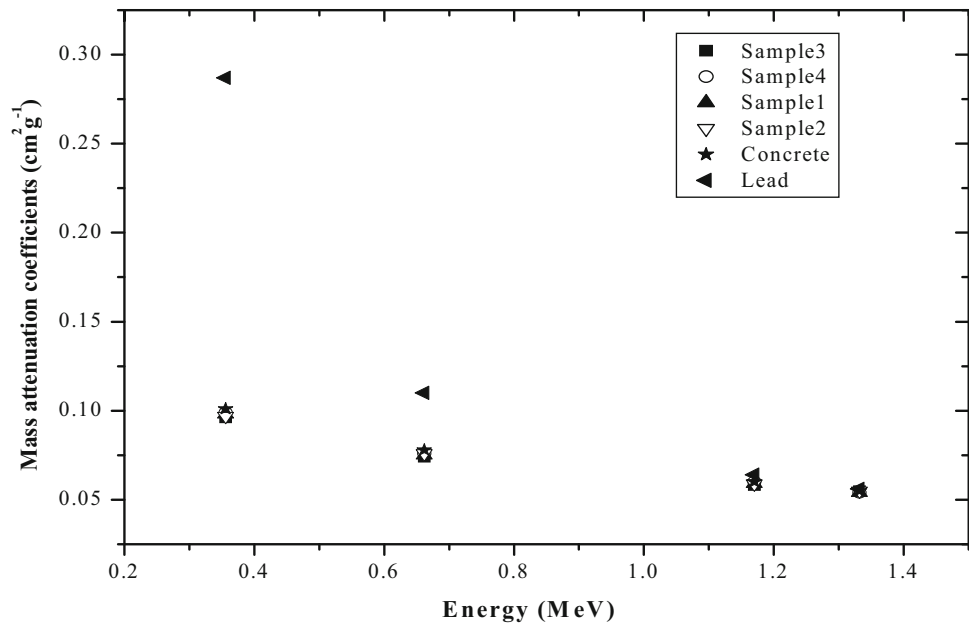


Table 5 Percentage difference of mass attenuation coefficients of the olive peat (M, K, A, and I) samples with respect to the calculated XCOM for concrete

Energy (MeV)	Samples			
	M	K	A	I
0.059	– 11.16	– 6.05	– 6.05	– 10.62
0.356	– 0.50	– 0.30	– 0.30	– 0.70
0.662	– 0.46	– 0.30	– 0.30	– 0.37
1.17	– 0.39	– 0.56	– 0.53	– 0.44
1.332	– 0.30	– 0.20	– 0.20	– 0.10

Table 7 Experimental and calculated values of HVL (cm) for olive peat (M, K, A, and I) samples and calculated values of concrete and lead at 0.059, 0.356, 0.662, 1.17, and 1.332 MeV photon energies

Energy (MeV)	Samples					
	M	K	A	I	Concrete	Lead
0.059	3.37	2.45	2.95	3.35	1.07	0.01
0.356	5.95	5.51	6.31	6.24	2.97	0.21
0.662	7.78	7.20	8.09	7.90	3.87	0.56
1.17	10.18	9.87	10.16	10.54	5.00	0.96
1.332	10.98	10.19	11.31	10.86	5.48	1.09

Table 6 Comparison of the mass attenuation coefficient results of the olive peat (M, K, A, and I) samples and calculated concrete and polymer materials from previous studies Abdel-Rahman et al. [23], Singh et al. [24], Kucuk et al. [25]

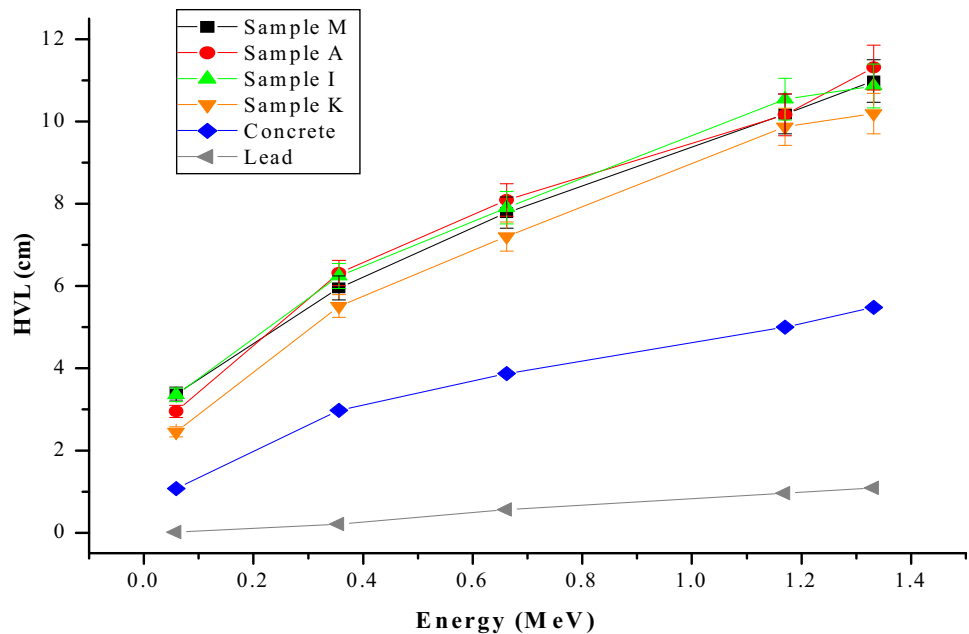
Energy MeV	Samples							
	Measured concrete	M	K	A	I	Perspex ^a	Polyethylene ^b	Polycarbonate ^c
0.059	0.281	0.169 ± 0.019	0.221 ± 0.020	0.203 ± 0.017	0.175 ± 0.016	0.193 ^a	0.112 ^b	0.172 ^c
0.356	0.101	0.096 ± 0.012	0.098 ± 0.017	0.095 ± 0.011	0.094 ± 0.013	–	–	–
0.662	0.078	0.073 ± 0.008	0.075 ± 0.006	0.074 ± 0.006	0.074 ± 0.004	0.084 ^a	0.072 ^b	0.081 ^c
1.17	0.060	0.056 ± 0.004	0.058 ± 0.005	0.055 ± 0.003	0.056 ± 0.004	–	0.054 ^b	0.061 ^c
1.332	0.055	0.052 ± 0.003	0.053 ± 0.003	0.053 ± 0.002	0.054 ± 0.003	0.060 ^a	0.056 ^b	0.057 ^c
Density (g/ cm ³)	2.30	1.21	1.28	1.16	1.18	1.18 ^a	0.92 ^b	1.22 ^c

^aAbdel-Rahman et al. [23]

^bKucuk et al. [25]

^cSingh et al. [24]

Fig. 7 (Color online) The HVL results of olive peat (M, K, A, and I) samples and calculated concrete and lead



with the calculated HVL of concrete and Pb. The HVL values of the samples increase with increasing photon energy. According to their, HVL the olive peat samples, concrete, and Pb exhibit the same behavior. HVL is an important quantitative factor of the penetration potential of specific radiation through specific materials [26]. Materials with values lower than HVL are better radiation shields in terms of thickness requirements [27]. Figure 7 shows that the HVL of Pb and concrete is minimal due to their high density. By comparison, the HVL of the olive peat samples indicates lower shielding effectiveness than that of concrete. Therefore, to achieve the required radiation protection, a thicker layer of olive peat should be applied.

4 Conclusion

The present study revealed the μ/ρ of olive peat samples obtained from four different regions in Jordan at photon energies of 0.059, 0.356, 0.662, 1.17, and 1.332 MeV. Radioactive ^{214}Am , ^{133}Ba , ^{137}Cs , and ^{60}Co point sources were used. The results indicated that the μ/ρ of olive peat samples is in good agreement with the calculated μ/ρ of concrete with an estimated error of only 1.8–6.9% at photon energies of 0.356–1.332 MeV. In particular, the μ/ρ of the olive peat samples was closer to the calculated μ/ρ of concrete than to that of Pb at 0.356 MeV. These findings indicate that olive peat has potential use in radiation applications in the field of medical physics. The HVL of all samples was measured, and the olive peat samples revealed lower shielding effectiveness than concrete. Olive peat is a natural and easily available material.

Acknowledgements The author would like to thank Dr. Hajo Idriss Mohammad (Sudan Atomic Energy Commission) for providing assistance in obtaining the elemental composition of the olive peat samples by energy-dispersive X-ray analysis.

References

- O. Al-Ketan, Potential of using olive pomace as a source of renewable energy for electricity generation in the Kingdom of Jordan. *J. Renew. Sustain. Energy* **4**, 063132 (2012). <https://doi.org/10.1063/1.4769205>
- F. Ceglie, H. Elshafie, V. Verrastro et al., Evaluation of olive pomace and green waste composts as peat substitutes for organic tomato seedling production. *Compost. Sci. Util.* **19**, 293–300 (2011). <https://doi.org/10.1080/1065657X.2011.10737011>
- I. Rotherham, *Peat and Peat Cutting* (Bloomsbury Publishing, London, 2011). (ISBN: 9780747807056)
- A. Madi, L. Kuraan, *Jordan Olive Monthly Report* (National Centre for Agricultural Research and Technology Transfer, Amman, 1999)
- I. Salinas, C. Conti, R. Lopes, Effective density and mass attenuation coefficient for building material in Brazil. *Appl. Radiat. Isot.* **64**, 13–18 (2006). <https://doi.org/10.1016/j.apradiso.2005.07.003>
- K.S. Mann, B. Kaur, G.S. Sidhu et al., Investigations of some building materials for γ -rays shielding effectiveness. *Radiat. Phys. Chem.* **87**, 16–25 (2013). <https://doi.org/10.1016/j.radphyschem.2013.02.012>
- K. Satoh, N. Ohashi, H. Higuchi et al., Determination of attenuation coefficient for self-absorption correction in routine gamma ray spectrometry of environmental bulk sample. *J. Radioanal. Nucl. Chem.* **84**, 431–440 (1984). <https://doi.org/10.1007/BF02036983>
- M. Sayyed, F. Akman, I. Geçibesler et al., Measurement of mass attenuation coefficients, effective atomic numbers, and electron densities for different parts of medicinal aromatic plants in low-energy region. *Nucl. Sci. Technol.* **29**, 144 (2018). <https://doi.org/10.1007/s41365-018-0475-0>

9. H.O. Tekin, E.E. Altunsoy, T. Manici et al., Mass attenuation coefficients of human body organs using MCNPX Monte Carlo code. *Iran. J. Med. Phys.* **14**, 229–240 (2017). <https://doi.org/10.22038/IJMP.2017.23478.1230>
10. H.O. Tekin, M. Karahan, T.T. Erguzel et al., Radiation shielding parameters of some antioxidants using Monte Carlo method. *J. Biol. Phys.* **44**, 579–590 (2018). <https://doi.org/10.1007/s10867-018-9507-6>
11. H. Tekin, M. Sayyed, O. Kilicoglu et al., Calculation of gamma-ray attenuation properties of some antioxidants using Monte Carlo simulation method. *Biomed. Phys. Eng. Express* **4**, 057001 (2018). <https://doi.org/10.1088/2057-1976/aad297>
12. A. Abdo, M. Ali, M. Ismail, Natural fibre high-density polyethylene and lead oxide composites for radiation shielding. *Radiat. Phys. Chem.* **66**, 185–195 (2003). [https://doi.org/10.1016/S0969-806X\(02\)00470-X](https://doi.org/10.1016/S0969-806X(02)00470-X)
13. I. Akkurt, R. Altindag, T. Onargan et al., The properties of various igneous rocks for γ -ray shielding. *Constr. Build. Mater.* **21**, 2078–2082 (2007). <https://doi.org/10.1016/j.conbuildmat.2006.05.059>
14. J. Osborn, T. Ersez, G. Braoudakis, Radiation shielding design for neutron diffractometers assisted by Monte Carlo methods. *Phys. B Condens. Matter* **385**, 1321–1323 (2006). <https://doi.org/10.1016/j.physb.2006.06.064>
15. C. Zeitlin, S. Guetersloh, L. Heilbronn et al., Measurements of materials shielding properties with 1 GeV/nuc ^{56}Fe . *Nucl. Instrum. Methods Phys. Res. Sect. B* **252**, 308–318 (2006). <https://doi.org/10.1016/j.nimb.2006.08.011>
16. I.F. Al-Hamarneh, M.W. Marashdeh, F.I. Almasoud et al., Determination of gamma-ray parameters for polyethylene glycol of different molecular weights. *Nucl. Sci. Technol.* **28**, 157 (2017). <https://doi.org/10.1007/s41365-017-0311-y>
17. A. El-Sersy, A. Hussein, H. El-Samman et al., Mass attenuation coefficients of $\text{B}_2\text{O}_3\text{--Al}_2\text{O}_3\text{--SiO}_2\text{--CaF}_2$ glass system at 0.662 and 1.25 MeV gamma energies. *J. Radioanal. Nucl. Chem.* **288**, 65–69 (2011). <https://doi.org/10.1007/s10967-010-0924-7>
18. I. Akkurt, Effective atomic and electron numbers of some steels at different energies. *Ann. Nucl. Energy* **36**, 1702–1705 (2009). <https://doi.org/10.1016/j.anucene.2009.09.005>
19. I. Akkurt, C. Basyigit, S. Kilincarslan et al., Radiation shielding of concretes containing different aggregates. *Cem. Concr. Compos.* **28**, 153–157 (2006). <https://doi.org/10.1016/j.cemconcomp.2005.09.006>
20. ICRU Report 33, Radiation Quantities and Units Pub: International Commission on Radiation Units and Measurements. Washington, DC (1980). <https://doi.org/10.1002/jlcr.2580180918>
21. I. Akkurt, H. Akyildirim, B. Mavi et al., Photon attenuation coefficients of concrete includes barite in different rate. *Ann. Nucl. Energy* **37**, 910–914 (2010). <https://doi.org/10.1016/j.anucene.2010.04.001>
22. M. Berger, J. Hubbell, S. Seltzer et al., XCOM: photon cross sections database, NIST standard reference database 8 (XGAM) (2010). <https://doi.org/10.18434/t48g6x>
23. M. Abdel-Rahman, E. Badawi, Y. Abdel-Hady et al., Effect of sample thickness on the measured mass attenuation coefficients of some compounds and elements for 59.54, 661.6 and 1332.5 keV γ -rays. *Nucl. Instrum. Methods. Phys. Res. Sect. A* **447**, 432–436 (2000). [https://doi.org/10.1016/S0168-9002\(99\)01257-7](https://doi.org/10.1016/S0168-9002(99)01257-7)
24. V. Singh, S. Shirmardi, M. Medhat et al., Determination of mass attenuation coefficient for some polymers using Monte Carlo simulation. *Vacuum* **119**, 284–288 (2015). <https://doi.org/10.1016/j.vacuum.2015.06.006>
25. N. Kucuk, M. Cakir, N. Isitman, Mass attenuation coefficients, effective atomic numbers and effective electron densities for some polymers. *Radiat. Prot. Dosim.* **153**, 127–134 (2012). <https://doi.org/10.1093/rpd/ncs091>
26. A. Akkas, Determination of the tenth and half value layer thickness of concretes with different densities. *Acta Phys. Pol. A* **1294**, 770–772 (2016). <https://doi.org/10.12693/APhysPolA.129.770>
27. H. Mann, G. Brar, K. Mann et al., Experimental investigation of clay fly ash bricks for gamma-ray shielding. *Nucl. Eng. Technol.* **48**, 1230–1236 (2016). <https://doi.org/10.1016/j.net.2016.04.001>